Mechanism and Dynamic Correlation Effects in Cycloaddition Reactions of Singlet Difluorocarbene to Alkenes and Disilene

Xingfa Gao, Yuhki Ohtsuka, Kazuya Ishimura, and Shigeru Nagase*

Department of Theoretical and Computational Molecular Science, Institute for Molecular Science, Myodaiji, Okazaki 444-8585, Japan

Received: February 20, 2009; Revised Manuscript Received: July 27, 2009

Mechanisms of the cycloaddition reactions of singlet difluorocarbene (CF_2) to alkenes and disilene were studied using CASSCF, MR-MP2, CR-CC(2,3), and UB3LYP methods in combination with basis sets up to 6-311++G(3d,p). The CASSCF(4,4) energies suggest that the cycloadditions all follow the stepwise mechanism. However, energies calculated using the MR-MP2(4,4) and CR-CC(2,3) methods in combination with the 6-311G(d) or larger basis sets consistently show that the reactions follow a concerted mechanism. The stepwise mechanisms predicted at the CASSCF level are "artificial" because of their neglect of dynamic electron correlation effects. The importance of dynamic electron correlation in determining the mechanistic nature of the reactions is explained through knowledge of the reacting system's geometries and charges along the reaction path.

Introduction

The [2 + 1] thermal cycloaddition between singlet carbenes and alkenes has been widely used in organic chemistry for the synthesis of three-membered rings.[1−7] This reaction's mechanism has attracted great attention over the past half century.[8−16] In this reaction, two new carbon−carbon σ bonds are created between the reactants. A number of computational studies have revealed that these two bonds' formation is an asynchronous process that is classifiable into two phases. The first phase involves the electrophilic interaction of the vacant p-like orbital (i.e., LUMO) of the carbene with the filled π orbital (i.e., HOMO) of the alkene, which mainly contributes to the formation of the first bond. The second phase involves the nucleophilic interaction of the filled σ-like orbital (i.e., HOMO) of the carbene with the vacant π^* orbital (i.e., LUMO) of the alkene, which mainly contributes to the formation of the other bond and accomplishes the reaction.[8−16] The adoption of such an asynchronous mode of bond formation is known to be directly related to the orbital symmetry rules, which implies that the synchronic creation of both bonds is "orbital-symmetry forbidden".[10]

Unlike the asynchronous nature of the cycloaddition, which has been well documented,[8−20] a discrepancy has long been recognized in the number of steps involved in the reaction. Calculations using spin-restricted single-determinant wave function models have consistently predicted that the cycloaddition of singlet carbenes to alkenes occurs via a one-step (concerted) mechanism, that is, path 1 or 2. (See Scheme 1.) Calculations using multireference wave function models or spin-unrestricted single-determinant wave function models have predicted that the selection between the one-step and two-step mechanisms occurs case-by-case and that some cycloadditions do follow the two-step mechanism, that is, path 3 instead of path 1 or 2. (See Scheme 1.)

In 1980, Houk et al.[11] investigated the cycloadditions of singlet CF_2, CCl_2, CFOH, and $C(OH)_2$ to alkenes for the first time using an ab initio approach, with the spin-restricted HF (RHF) method in combination with the STO-3G basis set. They found that all of these reactions follow a concerted mechanism. Such a concerted mechanism has been supported by a number of subsequent studies of the cycloadditions of carbenes to other alkenes or alkene-related substrates using spin-restricted density functional theory (DFT) methods in combination with much larger basis sets.[12−18] In 1997, Bernardi et al.[19] reinvestigated

SCHEME 1: Possible Reaction Mechanisms for the [2 + 1] Cycloadditions of Singlet Carbenes to Alkenes[a]

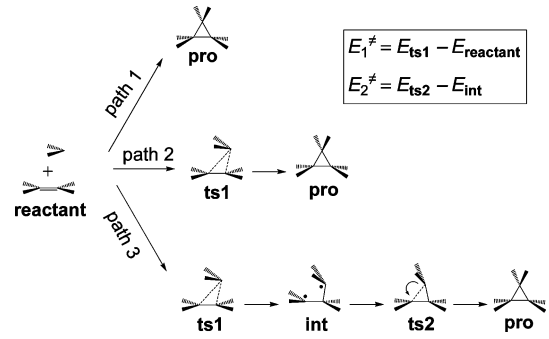

[a] In path 3, the black circles of **int** represent radical electrons. The arrow of **ts2** indicates the direction of ring closure. The inset shows definitions of the reaction energy barriers ($E_1^{\neq}$ and $E_2^{\neq}$) involved in the paths.

CHART 1: Six Substrates: Ethylene (1), Isobutene (2), Methylenecyclopropane (3), Propan-2-ylidene-cyclopropane (4), Bicyclopropylidene (5), and Disilene (6)[a]

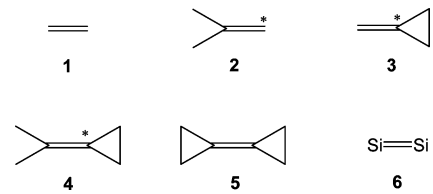

[a] Star (*) signifies the carbon atom of the substrate being attacked by CF_2 in the cycloaddition reaction studied here.

* Corresponding author. E-mail: nagase@ims.ac.jp.

10.1021/jp901553y CCC: $40.75
Published on Web 08/17/2009

CHART 2: Definitions of Active Spaces for the Reaction Systems

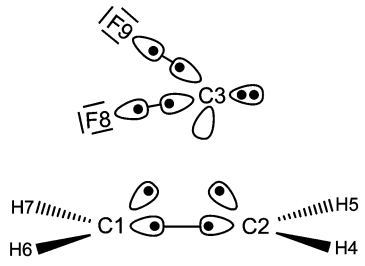

CAS(4,4): HOMO(CF_2), LUMO(CF_2), $\pi(C_2H_4)$, $\pi^*(C_2H_4)$

CAS(8,8): $\sigma(CF_2)$, $\pi(CF_2)$, $\pi(C_2H_4)$, $\pi^*(C_2H_4)$
σ(C3–F8), σ^*(C3–F8), σ(C3–F9), σ^*(C3–F9)

CAS(10,10): $\sigma(CF_2)$, $\pi(CF_2)$, $\pi(C_2H_4)$, $\pi^*(C_2H_4)$
σ(C3–F8), σ^*(C3–F8), σ(C3–F9), σ^*(C3–F9)
σ(C1–C2), σ^*(C1–C2)

the reactions of singlet CF_2 and $C(OH)_2$ with alkenes using two multireference methods, the complete active space self-consistent field (CASSCF) and the perturbative multireference MP2 (MR-MP2), in combination with two basis sets, 4-31G and 6-31G(d), respectively. In sharp contrast with the concerted mechanism predicted by Houk et al.,[11−18] their CASSCF results showed that the cycloadditions of both carbenes to ethylene or isobutene follow the stepwise mechanism (path 3) with a singlet diradical intermediate and with the second reaction energy barrier $E_2^{\ddagger}$ of 0.1−5.7 kcal/mol. (For the definition of $E_2^{\ddagger}$, see Scheme 1.) According to their MR-MP2 single-point (SP) energies, such a stepwise mechanism for the additions of both carbenes to ethylene turns out to be "artificial", which becomes concerted (i.e., path 2) after the inclusion of dynamic electron correlation effects at the MR-MP2 level, but the two-step path for the reaction "CF_2 + isobutene" does survive. In 2006, Bettinger[20] studied the cycloaddition of singlet CCl_2 to the models of the single-walled carbon nanotube (SWNT) using two different methods, spin-unrestricted B3LYP (UB3LYP) and perfect-pairing generalized valence bond (GVB-PP), in conjunction with the 6-31G(d) and 6-311G(d,p) basis sets. Similar to the multireference results,[19] his calculations showed that the addition of CCl_2 to the SWNT models also occurs via the two-step diradical mechanism with $E_2^{\ddagger} \approx 4.0$ kcal/mol. Single-determinant wave function models are well-known to have primary insufficiency in treating singlet diradical species. Therefore, the characterization of the diradical nature by Bernardi et al.[19] has constituted an important step forward for cycloaddition mechanisms involving carbenes and alkenes. Consequently, the two-step mechanism for the reaction "CF_2 + isobutene" obtained at the MR-MP2/6-31G(d) level of theory has become the fundamental exemplary proof for the existence of the stepwise mechanism. Because isobutene can be regarded as an alkene double bond substituted with two methyl groups, the results by Bernardi et al.[19] have led to a common belief that the cycloadditions of singlet carbenes to unsubstituted alkenes follow a concerted mechanism, path 1 or 2, whereas those to bulky substituted alkenes can follow the diradical stepwise mechanism, path 3.[15−20]

However, as shown by Bernardi et al.,[19] the inclusion of dynamic electron correlation effects into the CASSCF energies tends to reduce $E_2^{\ddagger}$ considerably. Therefore, it is desirable to know whether the stepwise path for the reaction "CF_2 + isobutene" survives when even larger basis sets are used, under the condition that the dynamic electron correlation is covered more adequately. A spin-unrestricted DFT (UDFT) approach has been widely used on many occasions because of its higher computational efficiency than those of the multireference wave function methods. Therefore, it is also worthwhile to examine the performance of UDFT methods in predicting the mechanisms for the titled reactions.

In the investigations described in this article, we examine mechanisms for cycloadditions of CF_2 to six substrates (i.e., **1**−**6** in Chart 1) using four methods, CASSCF, MR-MP2, UB3LYP, and completely renormalized coupled-cluster CR-CC(2,3), in conjunction with basis sets up to 6-311++G(3d,p). Results show that the CASSCF and UB3LYP methods do predict the stepwise mechanism, irrespective of the size of the basis set used. However, all of these stepwise paths, including that for the reaction "CF_2 + isobutene (**2**)", become concerted according to the energies obtained with the MR-MP2 and CR-CC(2,3) methods in combination with sufficiently large basis sets because of the adequate considerations of dynamic correlation effects. We report the reason for the importance of dynamic correlation effects in determining the reaction mechanisms, as obtained through studying the geometric changes and charge rearrangements during the cycloaddition of CF_2 to **1**. We also report the influences of basis sets on the calculated reaction mechanisms at the levels of CASSCF, MR-MP2, UB3LYP, and CR-CC(2,3) and the influences of active spaces on the calculated reaction mechanisms at the levels of CASSCF and MR-MP2.

Computational Details

The CASSCF method[21−25] was used for all geometry optimizations and frequency analyses; in these calculations, the active space consisting of four electrons, four active orbitals, that is, CAS(4,4), and the basis set 6-31G(d,p)[26−28] was applied. The definition of CAS(4,4) is the same as that given in an earlier study.[19] It consists of the π,π^* orbitals of the alkene and the HOMO and LUMO of CF_2. In other words, all structures, zero-point energies (ZPEs), and entropies reported in this article are at the CASSCF(4,4)/6-31G(d,p) level of theory.

The SP energies were calculated using four methods, CASSCF(4,4), MR-MP2(4,4),[29−31] CR-CC(2,3),[32−34] and UB3LYP,[35−37] in combination with basis sets ranging from 3-21G to 6-311++G(3d,p).[38−42] The MR-MP2 method includes a correction of dynamic electron correlation at the MP2 level to the CASSCF energies. Therefore, in principle, the accuracy of MR-MP2 energies will be greatly improved compared with the CASSCF energies. However, because the MR-MP2 only considers the dynamic correlation effects as a low-order perturbation, it yet poses the risk of overestimating the stabilities for some less-diradical structures that involve stronger dynamic correlation. In fact, CR-CC(2,3) is a new method designed for studying mechanisms of reactions with varying degrees of diradical character. Although it is a single-reference method, it can balance the nondynamic and dynamic electron correlation effects in the different stages of reactions reasonably well and can therefore accurately predict the reaction mechanisms. The accuracy of the CR-CC(2,3) method and its CR-CCSD(T) predecessor has been demonstrated by recent reports describing the [2 + 2]cycloaddition mechanism of cyclopentyne to **1**[43] and the isomerization mechanism of bicycle[1.1.0]butane.[44] Therefore, the simultaneous application of the CR-CC(2,3) method provides a valuable complement to the MR-MP2 results.[44]

To obtain the reaction energy profiles for the reaction "CF_2 + ethylene (**1**)", intrinsic reaction coordinate (IRC)[45−49] calculations were performed on the basis of the transition states (i.e.,

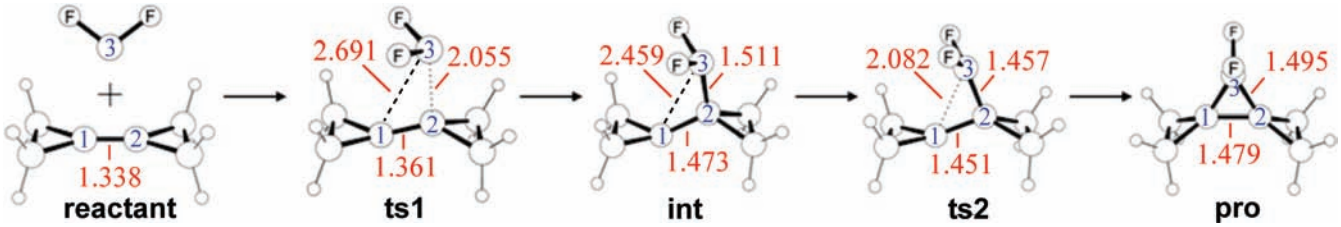

Figure 1. Stationary points for the reaction "CF_2 + **5**". The atomic distances (angstroms) between the carbon atom of CF_2 and those of the pristine double bond of **5** are labeled.

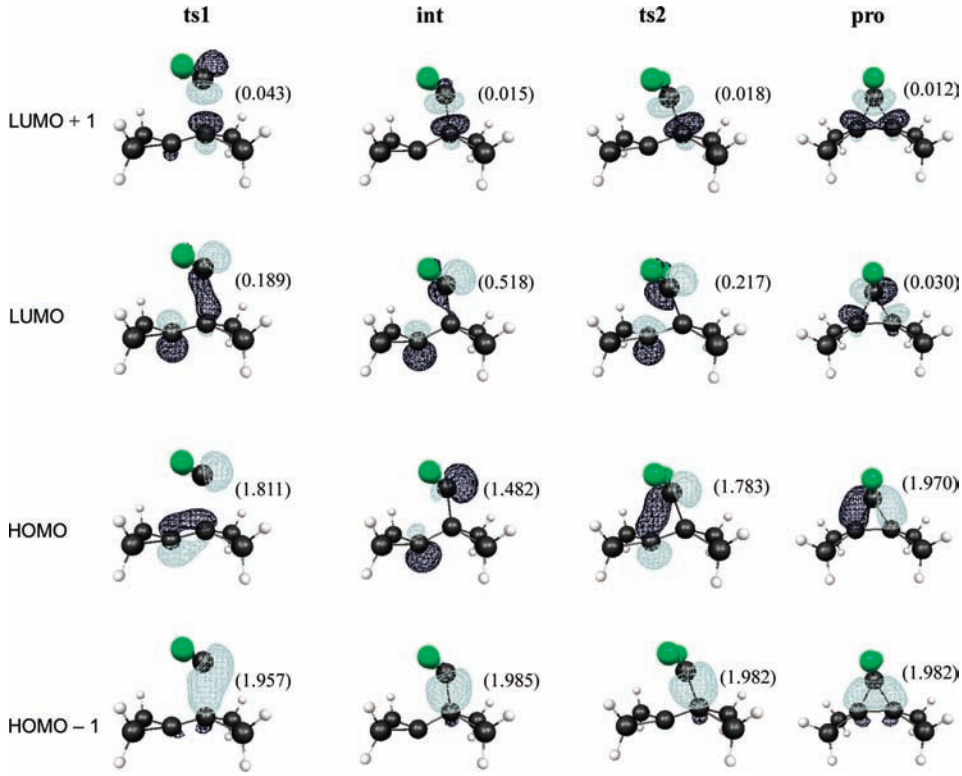

Figure 2. Orbitals included in the CASSCF(4,4)/6-31G(d,p) calculations for the reaction "CF_2 + **5**". Natural orbital occupation numbers (NOONs) are given in parentheses.

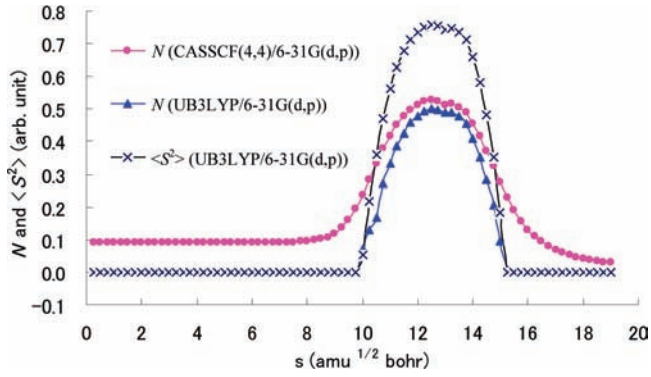

Figure 3. Degrees of diradical character (N) at the levels of CASSCF(4,4)/6-31G(d,p) and UB3LYP/6-31G(d,p) and the expected value of the S^2 operator ($\langle S^2 \rangle$) at the level of UB3LYP/6-31G(d,p) for the 76 structures along the reaction path of the reaction "CF_2 + **1**". These structures were located using IRC calculations at the CASSCF(4,4)/6-31G(d,p) level of theory. The "s" of abscissa represents the relative reaction steps. N were calculated using eq 1, whereas $\langle S^2 \rangle$ was obtained using SP calculations based on the CASSCF structures.

ts1 and **ts2**) of this reaction using the CASSCF(4,4)/6-31G(d,p) method and a step size of 0.25 amu$^{1/2}$ bohr. In all, 76 points (structures) along the reaction path were located. We obtained the reaction energy profile at the CASSCF(4,4)/6-31G(d,p) level by plotting the energies of the 76 points with respect to the steps. We obtained reaction energy profiles at other levels of theory by performing SP energy calculations based on these 76 structures. In addition to CAS(4,4), two other active spaces, CAS(8,8) and CAS(10,10) were also used; the definitions of these active spaces are portrayed in Chart 2.

The Gaussian 03 program[50] was used for the following calculations: geometry optimizations and frequency analyses for the stationary points, SP calculations at the levels of CASSCF,[21−25] MR-MP2,[30] (i.e., "CASSCF MP2" in Gaussian 03) and UB3LYP, and calculations of energy profiles at the level of UB3LYP. The GAMESS program[51] was used for the following calculations: IRC calculations, SP calculations at the level of CR-CC(2,3),[32,33] and calculations of energy profile at the levels of CASSCF, MR-MP2[31] (i.e., "MCQDPT"[52,53] in GAMESS) and CR-CC(2,3). The two multireference methods (i.e., "CASSCF MP2" in Gaussian 03 and "MCQDPT" in GAMESS) have similar characteristics but do not give exactly the same quantitative values. Multireference perturbation theories of both types concur: this means that the inclusion of dynamic correlation effects reduces the second energy barrier $E_2^{\ddagger}$. (See the Results and Discussion). The molecular orbitals were shown using the MacMolPlt program.[54]

TABLE 1: Relative Energies (E_{rel}, kilocalories per mole) with and without ZPE Corrections, Relative Gibbs Free Energies (G_{rel}, kilocalories per mole) and Entropies (S, calories per mole per Kelvin) for Stationary Points Calculated using Different Methods[a]

	CASSCF(4,4)[b]			MR-MP2(4,4)[b]			CR-CC(2,3)[c]			UB3LYP[b]			CASSCF(4,4)[b]
species	E_{rel}	E_{rel} + ZPE[d]	G_{rel}[e]	E_{rel}	E_{rel} + ZPE[d]	G_{rel}[e]	E_{rel}	E_{rel} + ZPE[d]	G_{rel}[e]	E_{rel}	E_{rel} + ZPE[d]	G_{rel}[e]	S
1 + CF_2	0.0	0.0	0.0	0.0	0.0	0.0	0.0	0.0	0.0	0.0	0.0	0.0	109.7
ts1	19.7	21.6	24.1	13.3	15.2	17.7	12.7	14.6	17.1	10.2	12.1	14.6	74.3
int	6.2	9.5	12.1	−2.5	0.8	3.4	4.1	7.4	10.0	0.9	4.2	6.8	72.8
ts2	8.3	11.3	14.1	−4.7	−1.7	1.1	0.8	3.8	6.6	0.5	3.6	6.4	70.9
pro	−37.7	−31.9	−29.0	−53.9	−48.1	−45.2	−47.9	−42.1	−39.2	−48.2	−42.4	−39.5	68.5
2 + CF_2	0.0	0.0	0.0	0.0	0.0	0.0	0.0	0.0	0.0	0.0	0.0	0.0	127.9
ts1	17.1	18.7	21.5	8.6	10.2	13.0	7.2	8.8	11.6	4.8	6.5	9.3	88.5
int	4.9	8.3	11.2	−7.0	−3.6	−0.7	−0.2	3.2	6.1	−2.1	1.3	4.2	86.8
ts2	9.6	12.4	15.4	−7.4	−4.6	−1.6	−1.4	1.4	4.4	−0.7	2.0	5.0	85.8
pro	−36.0	−31.0	−27.7	−53.2	−48.2	−44.9	−47.3	−42.3	−39.0	−44.9	−39.8	−36.5	81.6
3 + CF_2	0.0	0.0	0.0	0.0	0.0	0.0	0.0	0.0	0.0	0.0	0.0	0.0	121.8
ts1	17.2	18.5	21.2	11.0	12.3	15.0	8.9	10.2	12.9	8.3	9.7	12.4	83.5
int	−3.7	−0.9	2.0	−13.7	−10.9	−8.0	−6.7	−3.9	−1.0	−6.8	−4.0	−1.1	81.4
ts2	−1.3	1.1	4.1	−15.5	−13.1	−10.1	−9.9	−7.5	−4.5	−7.7	−5.3	−2.3	79.6
pro	−41.0	−35.7	−32.6	−56.8	−51.5	−48.4	−50.9	−45.6	−42.5	−49.6	−44.3	−41.2	77.8
4 + CF_2	0.0	0.0	0.0	0.0	0.0	0.0	0.0	0.0	0.0	0.0	0.0	0.0	137.3
ts1	14.1	15.5	18.3	5.3	6.7	9.5	2.8	4.2	7.0	2.4	3.8	6.6	97.6
int	−5.4	−2.2	0.8	−18.9	−15.7	−12.7	−11.5	−8.3	−5.3	−10.4	−7.2	−4.2	95.0
ts2	−0.2	2.2	5.2	−18.3	−15.9	−12.9	−12.4	−10.0	−7.0	−9.7	−7.2	−4.2	94.8
pro	−40.2	−35.2	−31.9	−57.1	−52.1	−48.8	−51.3	−46.3	−43.0	−47.3	−42.3	−39.0	91.0
5 + CF_2	0.0	0.0	0.0	0.0	0.0	0.0	0.0	0.0	0.0	0.0	0.0	0.0	132.7
ts1	14.3	15.8	18.6	6.6	8.1	10.9	4.0	5.5	8.3	4.0	5.5	8.3	92.8
int	−8.6	−5.0	−2.0	−20.3	−16.7	−13.7	−13.1	−9.5	−6.5	−11.5	−7.9	−4.9	90.5
ts2	−1.3	1.7	4.8	−19.9	−16.9	−13.8	−13.2	−10.2	−7.1	−10.6	−7.7	−4.6	88.5
pro	−45.3	−40.3	−37.0	−60.7	−55.7	−52.4	−55.2	−50.2	−46.9	−52.2	−47.2	−43.9	85.8
6 + CF_2	0.0	0.0	0.0	0.0	0.0	0.0	0.0	0.0	0.0	0.0	0.0	0.0	122.1
Ts1	2.5	3.6	5.9	−1.9	−0.8	1.5	−1.6	−0.5	1.8	−6.2	−5.0	−2.7	89.7
int	−25.2	−22.3	−19.6	−35.9	−33.0	−30.3	−27.4	−24.5	−21.8	−34.5	−31.5	−28.8	84.7
ts2	−21.0	−18.3	−15.3	−37.7	−35.0	−32.0	−28.2	−25.5	−22.5	−32.6	−29.9	−26.9	79.8
pro	−43.1	−39.3	−36.2	−58.1	−54.3	−51.2	−48.4	−44.6	−41.5	−53.7	−49.9	−46.8	79.0

[a] All data were calculated on the basis of geometries optimized at the CASSCF(4,4)/6-31G(d,p) level of theory. The SP energies were calculated using the 6-311+G(d,p) basis set. Zero-point energies (ZPEs) and entropies (S) are at the CASSCF(4,4)/6-31G(d,p) level. [b] Calculated using Gaussian 03 program. [c] Calculated using GAMESS program. [d] ZPEs unscaled. [e] Gibbs free energies at room temperature (298.15 K).

Results and Discussion

Reaction Mechanisms. Similar to the study by Bernardi et al.,[19] our geometry optimizations at the CASSCF(4,4)/6-31G(d,p) level of theory revealed four stationary points, that is, two local minima (**int**, **pro**) and two transition states (**ts1**, **ts2**), for the cycloaddition of CF_2 to each substrate. (See Chart 1.) For each cycloaddition, the stability order for these stationary points is **ts1** < **ts2** < **int** < **pro** at the same level of theory, suggesting that each cycloaddition follows a stepwise mechanism at this level.

To account for the reaction process, as an example, the structures **ts1**, **int**, **ts2**, and **pro**, which are associated in the reaction "CF_2 + **5**", are presented in Figure 1. According to Figure 1, the addition of CF_2 to **5** takes place in the way that the carbon atom of CF_2, that is, the atom labeled with number "3" (atom no. 3), first makes the bond with atom no. 2 of **5** and subsequently makes the bond with atom no. 1. As shown in Figure 1, the distance C3−C2 is shorter than distance C3−C1 in **ts1** or **int** or **ts2**, whereas both distances reach an equal number in **pro**. Such an asynchronous fashion of bond formation is consistent with the well-known result that the otherwise synchronous creation of both bonds is orbital-symmetry forbidden, which encounters a much higher reaction barrier energy.[10] Figure 2 shows active orbitals included in CAS(4,4) and the corresponding natural orbital occupation numbers (NOONs) obtained for the stationary points of the reaction "CF_2 + **5**". The NOONs for the HOMO and LUMO of **int** are, respectively, 1.482 and 0.518 (Figure 2), indicating that **int** has a profound diradical nature. For the addition of CF_2 to **1**−**4** or **6**, our calculations have revealed, respectively, similar diradical nature for the intermediate (**int**), with the corresponding NOONs of about 1.5 and 0.5 for the HOMO and LUMO. Therefore, our CASSCF(4,4)/6-31G(d,p) results predict that the additions of CF_2 to substrates **1**−**6** (Chart 1) all follow the stepwise diradical mechanism, path 3.

The degree of diradical character for a given structure can be evaluated using eq 1

$$N = 1 - (\mathrm{NOON_{HOMO}} - \mathrm{NOON_{LUMO}})/2 \qquad (1)$$

where N represents the degree of diradical character, and where $\mathrm{NOON_{HOMO}}$ and $\mathrm{NOON_{LUMO}}$ represent the NOONs of the HOMO and LUMO, respectively. Accordingly, a pure diradical has $N = 1$, whereas a closed-shell structure has $N = 0$.

To investigate how the degree of diradical character (N) changes during the reaction, Figure 3 depicts N for the 76 structures that are distributed along the reaction path of the reaction "CF_2 + **1**", which are located by IRC calculations at the level of CASSCF(4,4)/6-31G(d,p). Figure 3 shows that the value of N changes dramatically as the reaction proceeds; it obviously becomes larger in the region where the "s" of abscissa is 10−16 $\mathrm{amu}^{1/2}$ bohr (i.e., $10 < s < 16$). This region corresponds to the structural transition from **ts1** to **int** and then to **ts2**, which is critical for the creation of the new bonds. Furthermore, N has a shallow local minimum at the position where $s = 13$ $\mathrm{amu}^{1/2}$ bohr (Figure 3), which corresponds to the structure **int** in the reaction. Such a dramatic variation of the degree of diradical

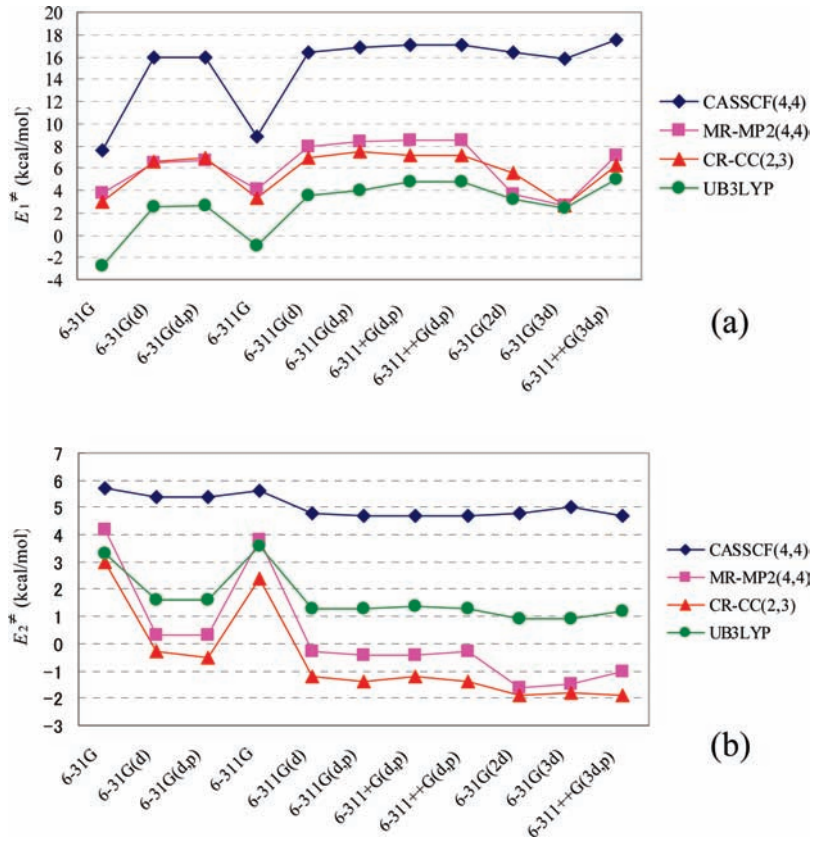

Figure 4. Variations of (a) $E_1^{\ddagger}$ and (b) $E_2^{\ddagger}$ with respect to basis set for the reaction "CF_2 + **2**". All energies are SP energies without ZPE corrections. For definitions of $E_1^{\ddagger}$ and $E_2^{\ddagger}$, see Scheme 1.

character along the reaction path implies that the influence of dynamic electron correlation on the calculated total energy is not constant at every point of the reaction path; in other words, the error caused by neglecting the dynamic electron correlation cannot be canceled out systematically. The CASSCF scheme does not cover the dynamic electron correlation. Therefore, the above stepwise mechanisms predicted by the CASSCF might be not conclusive.

Table 1 presents relative energies (E_{rel}), ZPE-corrected E_{rel}, and the relative Gibbs free energies (G_{rel}) calculated with the MR-MP2(4,4) and CR-CC(2,3) methods, in conjunction with the 6-311+G(d,p) basis set; those calculated with the CASSCF(4,4) and UB3LYP methods are also given for comparison. We consider the ZPE-corrected energies (i.e., E_{rel} + ZPE). For each cycloaddition, the CASSCF(4,4)/6-311+G(d,p) method predicts the same stepwise mechanism (i.e., path 3) as the CASSCF(4,4)/6-31G(d,p) does. (See Table 1.) In sharp contrast, the MR-MP2(4,4)/6-311+G(d,p) and CR-CC(2,3)/6-311+G(d,p) methods consistently predict a different stability order for the stationary points of each reaction, **ts1** < **int** < **ts2** < **pro**, which show that the energies decrease directly from **ts1** to **pro** (i.e., $E_2^{\ddagger} < 0$). The corresponding Gibbs free energies confirm such a decreasing order of energies. (See Table 1.) Taking the reaction "CF_2 + **5**" as an example, the ZPE-corrected energies at the CASSCF(4,4)/6-311+G(d,p) level predict $E_2^{\ddagger}$ to be 6.7 kcal/mol. However, the reaction turns out to be −0.2 and −0.7 kcal/mol, respectively, at the MR-MP2/6-311+G(d,p) and CR-CC(2,3)/6-311+G(d,p) levels of theory. (See Table 1.) In other words, the CASSCF method overestimates $E_2^{\ddagger}$ by about 7.0 kcal/mol. Comparing the energies obtained for other reactions, it is apparent that for each reaction, the $E_2^{\ddagger}$ calculated with the CASSCF method has been overestimated by an energy of 4.2−7.6 kcal/mol. A similar tendency of CASSCF to "overstabilize" singlet diradicals has been reported by several authors.[55−58] Regarding the first reaction energy barrier, the CASSCF(4,4)/6-311+G(d,p) results suggest that $E_1^{\ddagger}$ for the additions of CF_2 to **1**−**5** is 15.5−21.6 kcal/mol; it is 3.6 kcal/mol for the addition of CF_2 to **6**. However, the MR-MP2(4,4)/6-311+G(d,p) (or CR-CC(2,3)/6-311+G(d,p)) results suggest much smaller values for $E_1^{\ddagger}$: 6.7−15.2 (or 4.2−14.6) kcal/mol for the additions of CF_2 to **1**−**5** and is −0.8 (or −0.5) kcal/mol for the addition of CF_2 to **6**. Therefore, on the basis of these results, we conclude that the stepwise mechanisms predicted with the CASSCF(4,4) methods are "artificial" and that the cycloadditions of CF_2 to the six substrates of Chart 1 all take place via the concerted mechanism. Among them, the cycloadditions of CF_2 to **1**−**5** occur via path 2, whereas the addition of CF_2 to **6** occurs via path 1.

In an earlier study, Bernardi et al.[19] found that the addition of CF_2 to isobutene (**2**) follows a stepwise mechanism, although the addition of CF_2 to **1** follows a concerted mechanism, according to energies obtained at the level of MR-MP2(4,4)/6-31G(d). Actually, **2** has substituent groups (i.e., two methyl groups). Therefore, it has been generalized that the reactions of singlet CF_2 with unsubstituted alkenes follow the concerted mechanism, whereas those with bulky substituted alkenes can follow the stepwise mechanism. Among the six substrates we study here (Chart 1), **1**, **3**, and **6** are of the unsubstituted alkenes, whereas **2**, **4**, and **5** are of the substituted alkanes. However, as described above, all six reactions do follow the concerted mechanism according to the energies obtained using the MR-MP2 or CR-CC(2,3) method in conjunction with the larger basis set: 6-311+G(d,p). Therefore, the stepwise mechanism obtained at the MR-MP2(4,4)/6-31G(d) level[19] results from the small

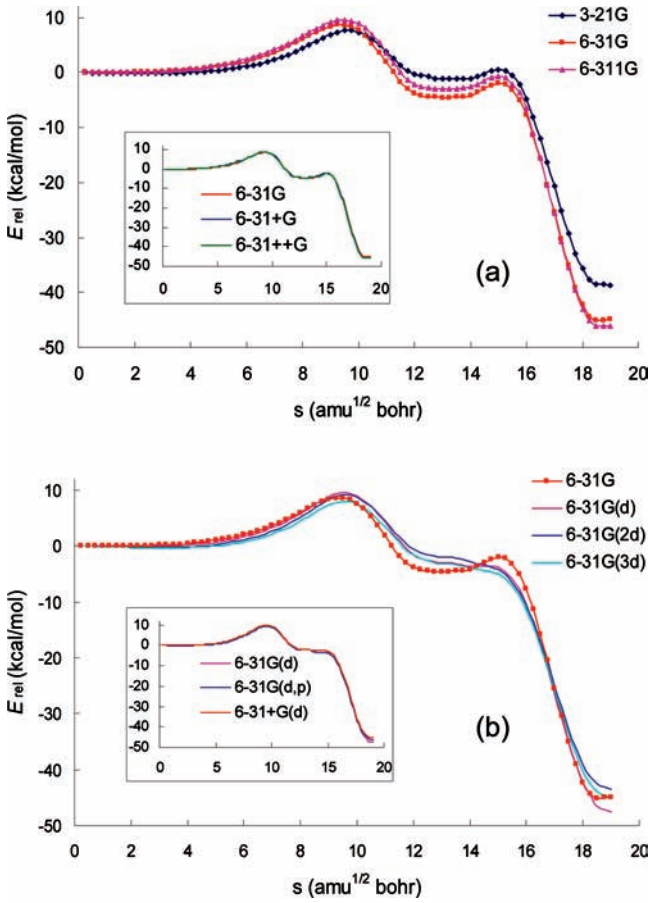

Figure 5. Reaction energy profiles for the reaction "CF_2 + **1**" calculated using the MR-MP2(4,4) method in combination with different basis sets. For the definition of "s" of the abscissa, see the caption of Figure 3. E_{rel} represents the SP energy of the point with respect to the SP energy of the point with $s = 0$.

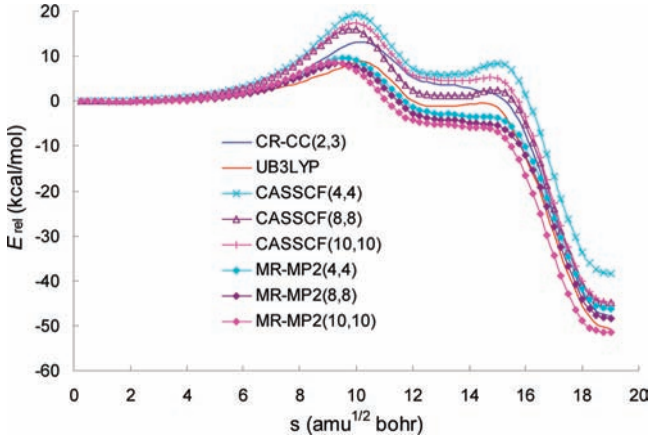

Figure 6. Energy profiles for the reaction "CF_2 + **1**" calculated using different methods in conjunction with the 6-31G(d,p) basis set. For the definition of "s" of the abscissa, see the caption of Figure 3; for the definition of the "E_{rel}", see the caption of Figure 5.

basis set, which is inadequate to consider the dynamic electron correlation effects; consequently, the stepwise mechanism proposed for the reactions of carbenes with substituted alkenes is doubtful.

The results obtained using the UB3LYP method are depicted in Figure 3 and Table 1. Figure 3 depicts the degree of diradical character (N) and the expectation value of the S^2 operator ($\langle S^2 \rangle$) for the addition of CF_2 to **1**, calculated with the UB3LYP/6-31G(d,p) method. N is 0.1 to 0.5, whereas $\langle S^2 \rangle$ is 0.05 to 0.75 in the region where $10 \leq s \leq 15$, which accords with the large degrees of the diradical character of this region, as revealed by the large N at the level of CASSCF(4,4)/6-31G(d,p); N and $\langle S^2 \rangle$ become zero in regions where $s < 10$ or $s > 15$, which is also compatible with the small degrees of diradical character therein at the CASSCF(4,4)/6-31G(d,p) level. (See Figure 3.) However, the UB3LYP method fails to predict the reaction mechanisms correctly. The energies at the level of UB3LYP/6-311+G(d,p) imply that the ZPE-uncorrected $E_2^{\ddagger}$ are 1.4, 0.7, 0.9, and 1.9 kcal/mol for the additions of CF_2 to **2**, **4**, **5**, and **6**, respectively, which are overestimated and which are qualitatively incorrect according to the MR-MP2(4,4) and CR-CC(2,3) results. (See Table 1.)

Influences of the Basis Set on the Calculated Reaction Mechanisms. We showed that both computational methods and basis sets are critical for correct predictions of the mechanisms for the titled reactions. To investigate further how the basis set size influences the performances of the methods and to find the smallest basis set that still yields reliable results, we calculated $E_1^{\ddagger}$ and $E_2^{\ddagger}$ for the cycloaddition of CF_2 to **2**, a substituted alkene, using the four methods in combination with 11 basis sets. We also calculated the reaction energy profile for the addition of CF_2 to **1**, an unsubstituted alkene, using the MR-MP2 method in combination with nine basis sets.

The $E_1^{\ddagger}$ and $E_2^{\ddagger}$ values obtained for the reaction "CF_2 + **2**" are presented in Figure 4. The corresponding numerical values are given in Table S2 of the Supporting Information. In Figure 4a,b, the four curves have generally similar shapes, which suggests that the variation of the basis set generally has similar influences on $E_1^{\ddagger}$ or $E_2^{\ddagger}$, independent of the applied computational methods. However, the curve corresponding to CASSCF(4,4) has the largest fluctuation in Figure 4a but the smallest fluctuation in Figure 4b. Because the CASSCF method considers nondynamic correlation effects but does not cover dynamic correlation effects, such different degrees of fluctuation probably indicate that the nondynamic correlation is more important, determining the mechanistic nature of the reaction in the early stage, that is, from **reactant** to **ts1**, whereas the dynamic correlation is more important, determining the mechanistic nature of the reaction in the late stage, that is, from **int** to **ts2**.

According to Figure 4b, the value of $E_2^{\ddagger}$ is always positive at the level of CASSCF(4,4) or UB3LYP, which corresponds to the existence of the "artificial" diradical intermediate. Therefore, we now discuss only the performances of the other two methods: MR-MP2(4,4) and CR-CC(2,3). Figure 4 shows that MR-MP2(4,4) and CR-CC(2,3) methods produce very close values for $E_1^{\ddagger}$ or $E_2^{\ddagger}$, no matter what variation of the basis set used. If we consider $E_1^{\ddagger}$ or $E_2^{\ddagger}$ obtained with the largest basis set, 6-311++G(3d,p), as the "true" result, then the following points can be drawn: (1) the use of one d-type polarization function, that is, enlarging the basis set from 6-31G to 6-31G(d), or from 6-311G to 6-311G(d), markedly improves the accuracy of $E_1^{\ddagger}$ and $E_2^{\ddagger}$ at the levels of MR-MP2(4,4) and CR-CC(2,3); (2) the use of split-valence, triple-ζ basis sets, that is, enlarging the basis set from 6-31G(d) to at least 6-311G(d), is critical for reducing $E_2^{\ddagger}$ from a positive value to a negative one and yields the concerted mechanism at the level of MR-MP2(4,4), although this does not simultaneously improve the accuracy of the $E_1^{\ddagger}$; (3) the further use of polarization or diffuse functions does not improve the accuracy of $E_1^{\ddagger}$ or $E_2^{\ddagger}$ considerably. Therefore, among the basis sets evaluated here, 6-311G(d) is the smallest that is appropriate for studying the mechanism of the reaction "CF_2 + **2**".

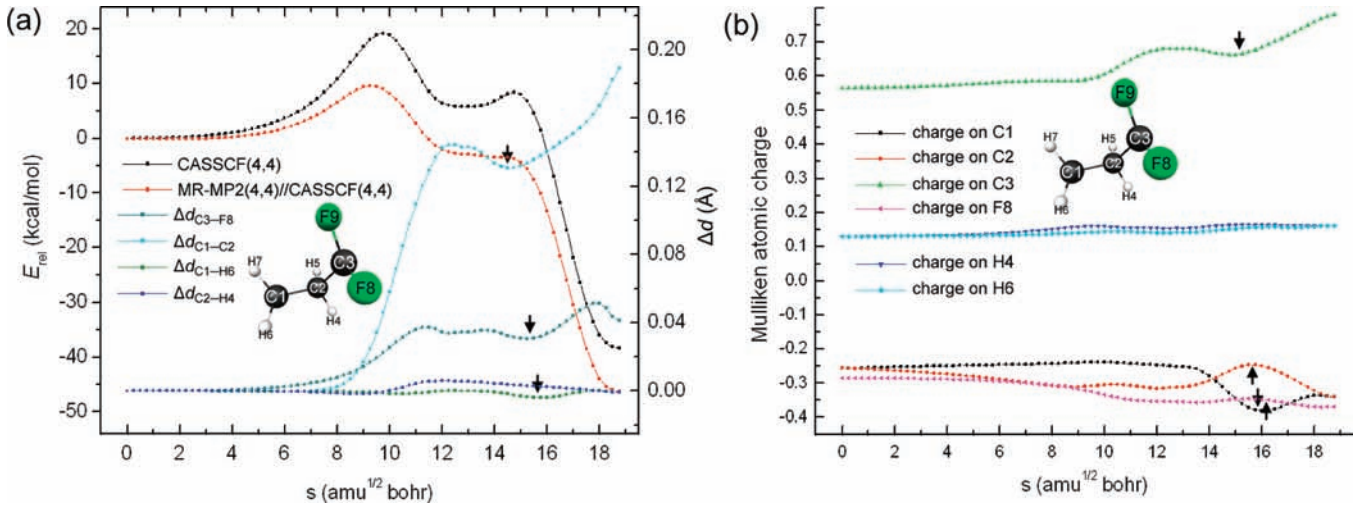

Figure 7. (a) Changes of bond lengths (Δd) along the reaction path for the reaction "CF_2 + **1**" at the level of CASSCF(4,4)/6-31G(d,p) and the reaction energy profiles at the levels of CASSCF(4,4)/6-31G(d,p) and MR-MP2(4,4)/6-31G(d,p)//CASSCF(4,4)/6-31G(d,p). At each point, $\Delta d = d - d_0$, where d represents the bond length at that point and where d_0 represents the bond length in the dissociated reactants. For the definition of "E_{rel}" of left ordinate, see the caption of Figure 5. (b) Charge distributions over the atoms during the cycloaddition at the level of CASSCF(4,4)/6-31G(d,p). For the definition of the "s" of abscissa of parts a and b, see the caption of Figure 3.

The results obtained for the reaction "CF_2 + **1**" are presented in Figure 5. As presented in Figure 5a, enlarging the basis set from 3-21G to 6-31G, 6-311G, 6-31+G, or 6-311+G fails to eliminate the existence of the "artificial" intermediate. However, as presented in Figure 5b, the use of one d-type polarization function (i.e., 6-31G(d)) works efficiently; the further application of polarization or diffuse functions to 6-31G(d) does not markedly alter the profile. Therefore, among the basis sets evaluated herein, 6-31G(d) is the smallest that is appropriate for studying the mechanism of the reaction "CF_2 + **1**". Nevertheless, because the 6-31G(d) basis set fails in the case of the reaction "CF_2 + **2**", we infer that 6-311G(d) is the smallest basis set that is appropriate for studying the mechanisms of cycloadditions involving general carbenes and alkenes.

Influences of Active Space on the Calculated Reaction Mechanisms. The CASSCF method is known to be very sensitive to the choice of active space. Therefore, we study how the change of active space influences the calculated reaction energy profiles. We calculated the reaction energy profiles for the reaction "CF_2 + **1**" using the CASSCF and MR-MP2 methods in combination with the 6-31G(d,p) basis set and with three different active spaces: CAS(4,4), CAS(8,8), and CAS(10,10). (For definitions of the active spaces, see Chart 2.) For comparison, we also calculated the reaction energy profiles at the levels of CR-CC(2,3)/6-31G(d,p) and UB3LYP/6-31G(d,p).

The obtained results are depicted in Figure 6. We first discuss the reaction energy profiles calculated using the CASSCF method in conjunction with the three active spaces. (See Figure 6.) The increase in the active space from CAS(4,4) to CAS(8,8) and further to CAS(10,10) flattens the shape of the CASSCF profile at the region where $13 < s < 15$ amu$^{1/2}$ bohr, which corresponds to the change of the structure from **int** to **ts2** in the reaction "CF_2 + **1**". Such an increase in active space does not dramatically change the shape of the profile at the region where $s < 10$ amu$^{1/2}$ bohr, which corresponds to the change of the structure from **reactant** to **ts1** in the reaction. At the CASSCF level, the strong or weak dependence of reaction energy profiles on the size of the active space that is used has been attributed to the greater or lesser importance of dynamic electron correlation effects involved in the reactions.[59,60] Therefore, Figure 6 demonstrates the importance of dynamic correlation effects in the reaction "CF_2 + **1**" when the structure changes from **int** to **ts2**, which is in agreement with our aforementioned point that the dynamic electron correlation dominates the mechanistic nature of the reaction "CF_2 + **2**" in the late stage. (See Figure 4 and the corresponding discussion.) The use of the three active spaces yields similar reaction energy profiles at the level of MR-MP2, suggesting that the active space of CAS(4,4) is adequate for studying the mechanisms of the titled reactions at the MR-MP2 level. As expected, CR-CC(2,3) also predicts the reaction energy profile correctly, although the UB3LYP method fails, predicting the stepwise mechanism. (See Figure 6.)

Reason for the Importance of Dynamic Correlation Effects. To study why dynamic electron correlation effects are so important in the late stages of the titled reactions and determine the stepwise mechanisms for these reactions, we analyzed the geometric changes and charge rearrangements along the reaction path for the reaction "CF_2 + **1**". As portrayed in Figure 7a, the bond lengths of C1−C2, C3−F8, C3−F7, C1−H6, and C1−H7 are reduced in the region where $13 < s < 17$ amu$^{1/2}$ bohr in the CASSCF energy profile; this region corresponds to the structural transition from **int** to **ts2** in the reaction; according to Figure 7b, in this region, the charge transfers from C1 and C3 to C2 and F8 (and F9). These results indicate that when the structure transforms from **int** to **ts2**, the electrons pass from C1 and C3 into the antibonding orbitals of C1−C2, C3−F8 (C3−F9), and C1−H6 (C1−H7), which instantaneously shortens the corresponding bond lengths and increases the importance of the dynamic correlation effects associated with these bonds. The structural transition from **int** to **ts2** fundamentally converts the singlet diradical to a closed-shell molecular system. Therefore, we have further studied a simpler reaction that converts a single diradical to a closed-shell molecular system, that is, "CF_2H + H → CF_2H_2". According to the results (Figure S2 of Supporting Information), it can be generalized by saying that as a reaction goes from a singlet radical to a closed-shell molecular system, the chemical bonds around the "radical centers" experience an instantaneous bond-shortening because of charge rearrangement, thereby increasing the dynamical correlation associated with these bonds.

Conclusions

The CASSCF(4,4) energies suggest that the cycloadditions of singlet CF_2 to alkenes (**1**−**5**) and disilene (**6**) all follow a stepwise mechanism (path 3), which is supported by the energies obtained using MR-MP2(4,4) and CR-CC(2,3) methods in combination with small basis sets. However, the energies calculated using the MR-MP2(4,4) and CR-CC(2,3) methods in combination with the 6-311G(d) or larger basis sets consistently suggest that each reaction follows the one-step concerted mechanism: the additions of CF_2 to alkenes **1**−**5** occur via path 2, whereas the addition of CF_2 to **6** occurs via path 1. The stepwise mechanisms predicted at the CASSCF level are "artificial" because of the neglect of dynamic electron correlation effects, although the stepwise mechanism is predicted using the MR-MP2 method with the smaller basis sets, which are inadequate to cover the dynamic correlation effects. Therefore, a point at which the cycloadditions of singlet carbenes to substituted alkenes can occur via the diradical stepwise mechanism is doubtful.

Among the four methods applied in this article, MR-MP2 and CR-CC(2,3) always correctly predict the reaction mechanisms, provided that sufficiently large basis sets are used, whereas the CASSCF always fails and the UB3LYP fails in some cases. The use of one d-type polarization function markedly improves the accuracy of the calculated relative energies. Among the basis sets evaluated, 6-311G(d) is the smallest that is appropriate for studying the mechanisms of the titled reactions using the MR-MP2 method, although the active space CAS(4,4) is adequate to this end. The important role of the dynamic correlation effects in determining the mechanisms of the reactions can be rationalized in terms of geometry variation and charge rearrangement during reaction processes.

Acknowledgment. We thank Dr. Michael W. Schmidt at Iowa State University for comments and improving the English language in the manuscript. We thank reviewer 2 for helpful comments. This work was supported by a Grant-in-Aid for Scientific Research on Priority Area and Next Generation Super Computing Project (Nanoscience Program) from MEXT of Japan.

Supporting Information Available: ZPEs and imaginary frequencies for all stationary structures, numerical values of the energy differences, vibration modes corresponding to the imaginary frequencies for the transition states associated in the reaction "CF_2 + 5", geometric changes and charge rearrangements during the reaction "CF_2H + H", Cartesian coordinates for all stationary structures, and Cartesian coordinates for the 76 structures distributed along the reaction path of "CF_2 + **1**". This material is available free of charge via the Internet at http://pubs.acs.org.

References and Notes

(1) A thematic issue of reviews on small rings and their chemistry, see: *Chem. Rev* **2003**, *103*, 4.
(2) Binger, P.; Büch, H. M. *Top. Curr. Chem.* **1987**, *135*, 77.
(3) Jennings, P. W.; Johnson, L. L. *Chem. Rev.* **1994**, *94*, 2241.
(4) de Meijere, A.; Kozhushkov, S. I. *Chem. Rev.* **2000**, *100*, 93.
(5) de Meijere, A.; Kozhushkov, S. I.; Schill, H. *Chem. Rev.* **2006**, *106*, 4926.
(6) Ma, S. M.; Zhang, J. L.; Cai, Y. J.; Lu, L. H. *J. Am. Chem. Soc.* **2003**, *125*, 13954.
(7) Ma, S. M.; Zhang, J. L. *J. Am. Chem. Soc.* **2003**, *125*, 12386.
(8) Skell, P. S.; Garner, A. Y. *J. Am. Chem. Soc.* **1956**, *78*, 5430.
(9) Moore, W. R.; Moser, W. R.; LaPrade, J. E. *J. Org. Chem.* **1963**, *28*, 2200.
(10) Hoffmann, R. *J. Am. Chem. Soc.* **1968**, *90*, 1475.
(11) Rondan, N. G.; Houk, K. N.; Moss, R. A. *J. Am. Chem. Soc.* **1980**, *102*, 1770.
(12) Houk, K. N.; Rondan, N. G.; Mareda, J. *J. Am. Chem. Soc.* **1984**, *106*, 4291.
(13) Blake, J. F.; Wierschke, S. G.; Jorgensen, W. L. *J. Am. Chem. Soc.* **1989**, *111*, 1919.
(14) Keating, A. E.; Garcia-Garibay, M. A.; Houk, K. N. *J. Am. Chem. Soc.* **1997**, *119*, 10805.
(15) Keating, A. E.; Merrigan, S. R.; Singleton, D. A.; Houk, K. N. *J. Am. Chem. Soc.* **1999**, *121*, 3933.
(16) Merrer, D. C.; Rablen, P. R. *J. Org. Chem.* **2005**, *70*, 1630.
(17) Lecea, B.; Ayerbe, M.; Arrieta, A.; Cossío, F. P.; Branchadell, V.; Ortuño, R. M.; Baceiredo, A. *J. Org. Chem.* **2007**, *72*, 357.
(18) Gao, X. F.; Ishimura, K.; Nagase, S.; Chen, Z. F. *J. Phys. Chem. A* **2009**, *113*, 3673.
(19) Bernardi, F.; Bottoni, A.; Canepa, C.; Olivucci, M.; Robb, M. A.; Tonachini, G. *J. Org. Chem.* **1997**, *62*, 2018.
(20) Bettinger, H. F. *Chem.—Eur. J.* **2006**, *12*, 4372.
(21) Cheung, L. M.; Sundberg, K. R.; Ruedenberg, K. *Int. J. Quantum Chem.* **1979**, *16*, 1103–1139.
(22) Roos, B. O.; Taylor, P. R.; Siegbahn, E. M. *Chem. Phys.* **1980**, *48*, 157.
(23) Ruedenberg, K.; Schmidt, M. W.; Gilbert, M. M.; Elbert, S. T. *Chem. Phys.* **1982**, *71*, 41.
(24) Roos, B. O. *Adv. Chem. Phys.* **1987**, *69*, 399.
(25) Schmidt, M. W.; Gordon, M. S. *Annu. Rev. Phys. Chem.* **1998**, *49*, 233.
(26) Hehre, W. J.; Ditchfield, R.; Pople, J. A. *J. Chem. Phys.* **1972**, *56*, 2257.
(27) Hariharan, P. C.; Pople, J. A. *Mol. Phys.* **1974**, *27*, 209.
(28) Francl, M. M.; Pietro, W. J.; Hehre, W. J.; Binkley, J. S.; Gordon, M. S.; DeFrees, D. J.; Pople, J. A. *J. Chem. Phys.* **1982**, *77*, 3654.
(29) Møller, C.; Plesset, M. S. *Phys. Rev.* **1934**, *46*, 618.
(30) McDouall, J. J.; Peasley, K.; Robb, M. A. *Chem. Phys. Lett.* **1988**, *148*, 183.
(31) Hirao, K. *Chem. Phys. Lett.* **1992**, *190*, 374.
(32) Piecuch, P.; Włoch, M. *J. Chem. Phys.* **2005**, *123*, 224105.
(33) Piecuch, P.; Włoch, M.; Gour, J. R.; Kinal, A. *Chem. Phys. Lett.* **2006**, *418*, 467.
(34) Piecuch, P.; Kucharski, S. A.; Kowalski, K.; Musiał, M. *Comput. Phys. Commun.* **2002**, *149*, 71.
(35) Becke, A. D. *Phys. Rev. A* **1988**, *38*, 3098.
(36) Lee, C.; Yang, W.; Parr, R. G. *Phys. Rev. B* **1988**, *37*, 785.
(37) Becke, A. D. *J. Chem. Phys.* **1993**, *98*, 5648.
(38) Krishnan, R.; Binkley, J. S.; Seeger, R.; Pople, J. A. *J. Chem. Phys.* **1980**, *72*, 650.
(39) McLean, A. D.; Chandler, G. S. *J. Chem. Phys.* **1980**, *72*, 5639.
(40) Clark, T.; Chandrasekhar, J.; Spitznagel, G. W.; Schleyer, P. v. R. *J. Comput. Chem.* **1983**, *4*, 294.
(41) Hariharan, P. C.; Pople, J. A. *Theor. Chim. Acta* **1973**, *28*, 213.
(42) Frisch, M. J.; Pople, J. A.; Binkley, J. S. *J. Chem. Phys.* **1984**, *80*, 3265.
(43) Kinal, A.; Piecuch, P. *J. Phys. Chem. A* **2006**, *110*, 367.
(44) Kinal, A.; Piecuch, P. *J. Phys. Chem. A* **2007**, *111*, 734.
(45) Ishida, K.; Morokuma, K.; Komornicki, A. *J. Chem. Phys.* **1977**, *66*, 2153.
(46) Muller, K. *Angew. Chem., Int. Ed.* **1980**, *19*, 1.
(47) Schmidt, M. W.; Gordon, M. S.; Dupuis, M. *J. Am. Chem. Soc.* **1985**, *107*, 2585.
(48) Garrett, B. C.; Redmon, M. J.; Steckler, R.; Truhlar, D. G.; Baldrige, K. K.; Bartol, D.; Schmidt, M. W.; Gordon, M. S. *J. Phys. Chem.* **1988**, *92*, 1476.
(49) Baldrige, K. K.; Gordon, M. S.; Steckler, R.; Truhlar, D. G. *J. Phys. Chem.* **1989**, *93*, 5107.
(50) Frisch, M. J.; Trucks, G. W.; Schlegel, H. B.; Scuseria, G. E.; Robb, M. A.; Cheeseman, J. R.; Montgomery, J. A., Jr.; Vreven, T.; Kudin, K. N.; Burant, J. C.; Millam, J. M.; Iyengar, S. S.; Tomasi, J.; Barone, V.; Mennucci, B.; Cossi, M.; Scalmani, G.; Rega, N.; Petersson, G. A.; Nakatsuji, H.; Hada, M.; Ehara, M.; Toyota, K.; Fukuda, R.; Hasegawa, J.; Ishida, M.; Nakajima, T.; Honda, Y.; Kitao, O.; Nakai, H.; Klene, M.; Li, X.; Knox, J. E.; Hratchian, H. P.; Cross, J. B.; Adamo, C.; Jaramillo, J.; Gomperts, R.; Stratmann, R. E.; Yazyev, O.; Austin, A. J.; Cammi, R.; Pomelli, C.; Ochterski, J. W.; Ayala, P. Y.; Morokuma, K.; Voth, G. A.; Salvador, P.; Dannenberg, J. J.; Zakrzewski, V. G.; Dapprich, S.; Daniels, A. D.; Strain, M. C.; Farkas, O.; Malick, D. K.; Rabuck, A. D.; Raghavachari, K.; Foresman, J. B.; Ortiz, J. V.; Cui, Q.; Baboul, A. G.; Clifford, S.; Cioslowski, J.; Stefanov, B. B.; Liu, G.; Liashenko, A.; Piskorz, P.; Komaromi, L.; Martin, R. L.; Fox, D. J.; Keith, T.; Al-Laham, M. A.; Peng, C. Y.; Nanayakkara, A.; Challacombe, M. P.; Gill, M. W.; Johnson, B. G.; Chen, W.; Wong, M. W.; Gonzalez, C.; Pople, J. A. *Gaussian03*, revision C.01; Gaussian, Inc.: Wallingford, CT, 2004.

(51) Schmidt, M. W.; Baldrige, K. K.; Boatz, J. A.; Elbert, S. T.; Gordon, M. S.; Jensen, J. H.; Koseki, S.; Matsunaga, N.; Dupuis, M.; Montgomery, J. A. *J. Comput. Chem.* **1993**, *14*, 1347.
(52) Nakano, H. *Chem. Phys. Lett.* **1993**, *207*, 372.
(53) Nakano, H. *J. Chem. Phys.* **1993**, *99*, 7983.
(54) Bode, B. M.; Gordon, M. S. *J. Mol. Graphics Modell.* **1998**, *16*, 133.
(55) Li, Y.; Houk, K. N. *J. Am. Chem. Soc.* **1993**, *115*, 7478.
(56) López, C. S.; Faza, O. N.; de Lera, Á. R. *Chem.—Eur. J.* **2007**, *13*, 5009.
(57) Guner, V.; Khuong, K. S.; Leach, A. G.; Lee, P. S.; Bartberger, M. D.; Houk, K. N. *J. Phys. Chem. A* **2003**, *107*, 11445.
(58) Lischka, H.; Ventura, E.; Dallos, M. *ChemPhysChem* **2004**, *5*, 1365.
(59) Forés, M.; Adamowicz, L. *J. Comput. Chem.* **1999**, *20*, 1422.
(60) Rovira, M. C.; Scheiner, S. *J. Phys. Chem.* **1995**, *99*, 9854.

JP901553Y